AGU100 ADVANCING EARTH AND SPACE SCIENCE

JGR

Journal of Geophysical Research: Oceans

RESEARCH ARTICLE
10.1029/2017JC013414

Does Pacific Variability Influence the Northwest Atlantic Shelf Temperature?

Ke Chen[1] and Young-Oh Kwon[1]

[1]Physical Oceanography Department, Woods Hole Oceanographic Institution, Woods Hole, MA, USA

Key Points:
- Statistically significant negative correlations exist between PDO and SST on the Northwest Atlantic shelf in spring and summer
- Atmospheric forcing dominates interannual variability of Northwest Atlantic shelf SST in spring, while oceanic forcing dominates in summer
- SST anomalies in the central and eastern North Pacific play a key role in these relationships

Correspondence to:
K. Chen,
kchen@whoi.edu

Citation:
Chen, K., & Kwon, Y.-O. (2018). Does Pacific variability influence the Northwest Atlantic shelf temperature? *Journal of Geophysical Research: Oceans*, *123*, 4110–4131. https://doi.org/10.1029/2017JC013414

Received 31 AUG 2017
Accepted 12 APR 2018
Accepted article online 19 APR 2018
Published online 28 JUN 2018

Abstract The relationship between North Pacific variability and sea surface temperature (SST) of the Northwest Atlantic continental shelf is examined over interannual time scale in 1982–2014. Statistically significant negative correlations exist between Pacific Decadal Oscillation (PDO) index and SST in the Gulf of Maine (GoM) in spring and summer. Cross-correlation analysis further suggests significant negative lead-lag correlations, with the spring PDO leading the GoM SST by 0–3 months while the summer PDO lags by 1–3 months. These correlations are dominated by the interannual component of the PDO. Statistical relationships are placed in context by further investigating the physical processes controlling the upper ocean mixed layer temperature budget in the GoM. The results reveal contrasting roles between the atmosphere and the ocean in spring and summer, respectively. Local atmospheric forcings, in particular the radiative air-sea fluxes, are the dominant driver for the interannual variability of springtime SST over the Northwest Atlantic shelf. In contrast, oceanic terms are important in controlling the interannual variability of summertime SST. As a result, reconstructed SST using atmospheric forcings successfully reproduces the statistical relationship with PDO in spring, but not in summer. Furthermore, it is shown that the SST anomalies in the central and eastern North Pacific play a key role in these relationships.

1. Introduction

With the global climate system undergoing rapid changes, it is important to understand how the global changes are impacting the coastal oceans, which have a direct relevance to human activities. This is particularly true for the Northwest Atlantic coastal ocean (Figure 1), which is a dynamic environment supporting highly productive ecosystem and some of the most commercially valuable fisheries. Growing evidence reveals the impact of climate change on the physical environment of the Northwest Atlantic coastal water in terms of both long-term trend (Forsyth et al., 2015; Pershing et al., 2015; Shearman & Lentz 2010) and extreme variability (Chen et al., 2014 2015). Associated with such physical changes are major shifts across the marine food web (e.g., Greene & Pershing 2007; Link & Ford, 2006; Lucey & Nye, 2010; Nye et al., 2009; Walsh et al., 2015), which further pose challenges to the ecosystem management (e.g., Mills et al., 2013; Pershing et al., 2015).

Large-scale atmospheric and oceanic indices are commonly used to find potential connections with processes over a wide spectrum of spatial scales. For example, the variability of local latitude of atmospheric jet stream was reported to have major impacts on the ocean temperature and ecosystem. Bane et al. (2007) and Barth et al. (2007) found that the intraseasonal oscillations of the atmospheric jet stream position can induce fluctuations in SST and ecosystem biomass in the costal ocean off Oregon. Similarly, Chen et al. (2014) suggested that in addition to the intraseasonal oscillations, the northward shift of jet stream latitude over seasonal time scale is the primary driver of the extreme warm anomalies over the Northwest Atlantic coastal ocean. Atmospheric blocking is likely the process behind the unusual jet stream variability (e.g., Santos et al., 2013). Another large-scale index, the North Atlantic Oscillation (NAO), which is the leading mode of the atmospheric variability in the North Atlantic sector (Hurrell, 1995), has been reported to be related to hydrographic conditions in the Gulf of Maine (GoM). Mountain (2012) using historical hydrographic data estimated the percentage of Labrador Slope Water (LSW) entering the GoM through the Northeast Channel, the deepest channel in the GoM, and compared the time series with the NAO index. More inflow of LSW into the GoM was found when the NAO index was low, with the NAO leading by 2 years. Xu et al. (2015) showed that the annual NAO index is negatively correlated with annual SST in the GoM 4 years later. They attributed the 4 year lag to the ocean advection along the Northwest Atlantic coast (e.g., Chapman &

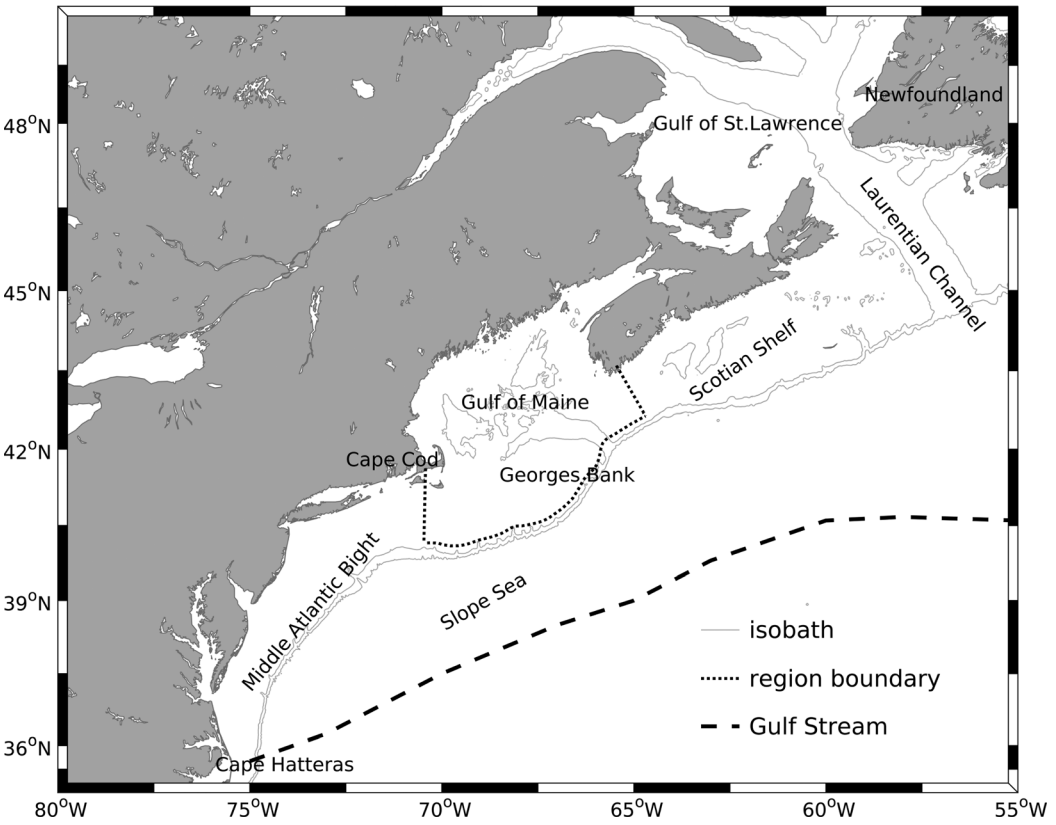

Figure 1. Map showing the Northwest Atlantic continental shelf region. The 200 and 1,000 m isobaths are contoured in light gray. The black-dotted line enclosed the Gulf of Maine region boundary used for the calculations in this work. The black-dashed line denotes the mean Gulf Stream location. Major geographic features are also labeled.

Beardsley, 1989). On the oceanic side, Peña-Molino and Joyce (2008) suggested that shifts of the Gulf Stream are associated with changes in the circulation and water mass properties of the Slope Water: colder waters are present when the circulation is more southwesterly and the Gulf Stream is to the south. Their result indicates a connection between slope circulation and the Gulf Stream. Along the same line, Nye et al. (2011) showed that the shifts of the Gulf Stream path are significantly correlated with the changes in the spatial distribution of silver hake on the Northwest Atlantic shelf. The argument is that these changes are both connected to the Atlantic meridional overturning circulation (AMOC), which modulates the Gulf Stream path, and the bottom temperature on the outer continental shelf (Joyce & Zhang, 2010; Peña-Molino & Joyce, 2008). Recently, Pershing et al. (2015) reported that seasonal mean GoM SST is significantly correlated with multiple large-scale indicators including Gulf Stream path, Atlantic Multidecadal Oscillation (AMO) and Pacific Decadal Oscillation (PDO). Based upon these relationships, they further developed multiple regression models to estimate summer SST in the GoM, which was used to better understand the changes in the Atlantic cod stock (Pershing et al., 2015). Considering the complexity of the atmosphere-ocean system and the varying proximity to the GoM, some of these significant correlations are remarkable (as further discussed in the following paragraph).

Better understanding of the mechanisms operating between large-scale forcing and regional-scale processes such as the variability of temperature in the Northwest Atlantic coastal ocean is scientifically important. While it is useful to compute correlations with the large-scale indices, the statistical relationships need be explained by physical mechanisms before any robust linkages can be established. One thing that is of particular interest to us is the reported significant correlation between the GoM SST and PDO index, which is −0.5/–0.67 in spring/summer during 1982–2013. This is a newly reported correlation, which is much stronger than those with AMO or NAO and is comparable to that with the Gulf Stream path index (Pershing et al., 2015). The PDO-GoM SST correlation being comparable to that of Gulf Stream path index-GoM SST is remarkable considering very different geographical and dynamical proximity of PDO and Gulf Stream to the

GoM. The PDO-GoM SST relationship is also intriguing as it might point to a connection between two ocean basins: PDO is a basin-wide SST signal in the North Pacific (see section 2) and GoM SST represents the surface thermal condition in the Northwest Atlantic coastal ocean. With both the scientific importance and the practical value, it is thus necessary to further examine this relationship.

In this work, we examine the relationship between the North Pacific variability represented by PDO and SST variability in the Northwest Atlantic coastal ocean, with a focus on identifying physical mechanisms. Specifically, we answer the following questions: Is there a robust connection between PDO and Northwest Atlantic SST? If so, what are the characteristics of this connection? More importantly, why does such a connection exist or does not exist, and what are the relevant physical processes? Addressing above questions will allow us to better understand the remote and local processes influencing the coastal ocean physical environment in a changing climate system. An improved understanding would certainly contribute to better ecosystem and fishery management.

In the following, we first introduce the methodology in section 2, and examine the statistical relationships between PDO and SST in the Northwest Atlantic coastal ocean in section 3. The targeted time scale is interannual, with seasonal dependence taken into consideration. Relevant atmospheric variables will also be analyzed. In section 4, we estimate the upper ocean mixed layer temperature budget, which can be used to quantitatively evaluate the potential connection. Discussions and summary can be found in section 5.

2. Methods and Data

2.1. Upper Ocean Mixed Layer Temperature Budget

We consider temperature budget diagnostics within the upper mixed layer to examine the role of atmospheric forcing and ocean advection on the interannual variability of Northwest Atlantic shelf SST, allowing us to investigate its potential physical linkages to the North Pacific variability. The temperature budget in the upper ocean can be estimated as follows:

$$\frac{\partial T}{\partial t}+\mathbf{u}\cdot\nabla T+w\frac{\partial T}{\partial z}-A_h\nabla^2 T+\frac{\partial}{\partial z}\overline{w'T'}=\frac{1}{\rho_0 C_p}\frac{\partial q}{\partial z} \tag{1}$$

Here T is the 4-dimensional temperature, $\mathbf{u}$ and w are horizontal and vertical velocities, A_h is the horizontal diffusivity, $\overline{w'T'}$ is vertical turbulent heat flux, ρ_0 is the average seawater density (1,024 kg m^{-3}), C_p is the specific heat capacity of seawater (3,985 J $kg^{-1}{}^{\circ}C^{-1}$), and q is the downward radiation flux. Neglecting horizontal diffusion, integration within the upper mixed layer yields:

$$\frac{\partial T_m}{\partial t}=\frac{Q_{net}-q_{-h_m}}{\rho_0 C_p h_m}-\mathbf{u}_m\cdot\nabla T_m-\frac{w_e\Delta T}{h_m} \tag{2}$$

Here T_m is the temperature within the mixed layer, Q_{net} is the net air-sea heat flux into the mixed layer, q_{-h_m} is the downward short-wave radiation flux at the base of the mixed layer, h_m is the mixed layer thickness, $\mathbf{u}_m$ is the average horizontal velocity vector in the mixed layer, w_e is the vertical velocity at the base of the mixed layer, and ΔT is the temperature difference between T_m and temperature just below the mixed layer.

To account for the changes of mixed layer depth $-h_m$, one element of the interannual variability in the upper ocean, we employ the Price-Weller-Pinkle (PWP) mixed layer model (Price et al., 1986) to estimate the time-varying mixed layer depth. The model requires an initial temperature/salinity profile, and steps forward in time with seven real-time atmospheric variables including turbulent (latent and sensible) and radiation (short and long-wave) fluxes, vector (eastward and northward) wind stress, and precipitation rate. The PWP model considers 1-D water column instability and mixing in response to surface heat, freshwater, and momentum fluxes. At each time step, the fluxes are applied to the top layer of the water column except for short-wave radiation, which is distributed over multiple layers. The water column then mixes from surface to depth to eliminate static instability. The model further considers entrainment below the initial mixed layer according to the Bulk Richardson Number criterion. In addition, the PWP model also considers instability below the mixed layer by ensuring Gradient Richardson Number greater than a critical value (0.25).

2.2. Data

2.2.1. Pacific Decadal Oscillation Index

Pacific Decadal Oscillation (PDO) is the year-round dominant pattern of North Pacific SST variability (Newman et al., 2016). It is defined as the leading empirical orthogonal function (EOF) mode of North Pacific

(20°–70°N) SST monthly anomalies, which are departures from the climatological annual cycle after removing the global mean SSTs (Mantua et al., 1997). The PDO index is available monthly from 1900 to present from the Joint Institute for the Study of the Atmosphere and Ocean (JISAO, http://research.jisao.washington.edu/pdo/). For sensitivity test, we also produced a 10 year high-pass filtered (using fifth-order Butterworth filter) PDO index.

2.2.2. Sea Surface Temperature and Air-Sea Flux Data

The satellite observation-based NOAA Optimum Interpolation (OI) 1/4° daily SST (AVHRR-only; Reynolds et al. (2007); http://www.ncdc.noaa.gov/oisst) since 1982 are primarily used due to its high spatial resolution, which is suited for the analyses of the continental shelf region. Therefore, our primary analysis period is 1982–2014. Additionally, the UK Met Office Hadley Centre Sea Ice and Sea Surface Temperature since 1870 (HadISST, 1° × 1°, https://www.metoffice.gov.uk/hadobs/hadisst/) is used. For the air-sea heat fluxes, three different data sets are used for parallel analysis of the temperature variability. The first data set is European Center Medium-Range Weather Forecasts (ECMWF) ERA-interim (Berrisford et al., 2011). Three-hourly turbulent (latent and sensible) and radiative (short-wave and long-wave) fluxes at a global 0.125° × 0.125° grid from 1979 to present are available (http://apps.ecmwf.int/datasets/data/interim-full-daily/levtype=sfc/). The second data set is National Centers for Environmental Prediction (NCEP) North American Regional Reanalysis (NARR) (Mesinger et al., 2006). Air-sea flux variables are available at 3 h interval from 1979 to 2014 with a 0.1875° × 0.1875° resolution(https://www.ncdc.noaa.gov/data-access/model-data/model-datasets/north-american-regional-reanalysis-narr). The third data set is Objectively Analyzed air-sea Fluxes (OAFlux) (Yu & Weller, 2007). Daily turbulent and radiation fluxes are available from 1985 to 2009 globally at a 1° × 1° grid (http://oaflux.whoi.edu/).

2.2.3. Forcing Variables for the PWP Model

To drive the PWP model, air-sea heat, freshwater, and momentum fluxes are needed. We examine three sets of forcings in parallel to evaluate the uncertainties in the data and to validate the conclusions. The first set of forcings is based on ERA-interim reanalysis, which includes heat fluxes, evaporation minus precipitation, and vector wind stress that was calculated from vector wind using formulas described by Large and Pond (1981). The second set of forcings is based on heat fluxes, precipitation, and vector wind from NARR and evaporation data from OAFlux. The third set of forcings is composed of heat fluxes and evaporation from OAFlux, 3 hourly precipitation from NARR, and 6 hourly, 1/4° vector wind data from the Cross-Calibrated Multi-Platform (CCMP) project. The initial profiles are temperature/salinity monthly climatology from World Ocean Atlas (WOA) 2013 version 2 at 1/4° × 1/4° resolution (https://www.nodc.noaa.gov/OC5/woa13/). The time-varying atmospheric variables are averaged to daily means before being used to force the PWP model. All variables are interpolated onto the 1/4° × 1/4° grid of OI SST.

3. Statistical Relationships With PDO

3.1. Correlation Between PDO and SST

Pershing et al. (2015) reported that the GoM SST (averaged within a geographic box) is significantly correlated with PDO in spring and summer over the interannual time scale. To learn about the spatial context of the correlation, we calculate the linear correlation between PDO index and SST over the Northwest Atlantic continental shelf for each season during 1982–2014 (Figure 2). Note that the statistical significance of the correlations are tested considering their autocorrelations (Emery & Thomson, 2001). In winter (January–February–March, JFM), correlations over the majority of the shelf were slightly negative, but no shelf-wide significant correlations were found. In spring (April–May–June, AMJ), significant negative correlations developed in the southwestern Gulf of St. Lawrence, Gulf of Maine, and shallower shelf of the Middle Atlantic Bight. The most negative correlation is about −0.59 in the central GoM, significant at 99% level. In summer (July–August–September, JAS), the negative correlations are more confined in the GoM. The negative correlations are even stronger, reaching a peak value of −0.66, significant at 99% level. There are also negative correlations in the Gulf of St. Lawrence with significant but weaker magnitudes. The strong negative correlations disappear in fall (October–November–December, OND). Note that repeating the above correlation analysis using HadISST (1° × 1°) for the same time period reveals similar results.

To search for potential lead/lag relationship, we calculated the cross correlation between 3 monthly (averaged over each 3 months) PDO index and GoM SST (polygon enclosed by the dashed line and the coastline in Figure 1) during 1982–2014 (Figure 3). Strong negative correlations between the two ($r = -0.4 \sim -0.6$)

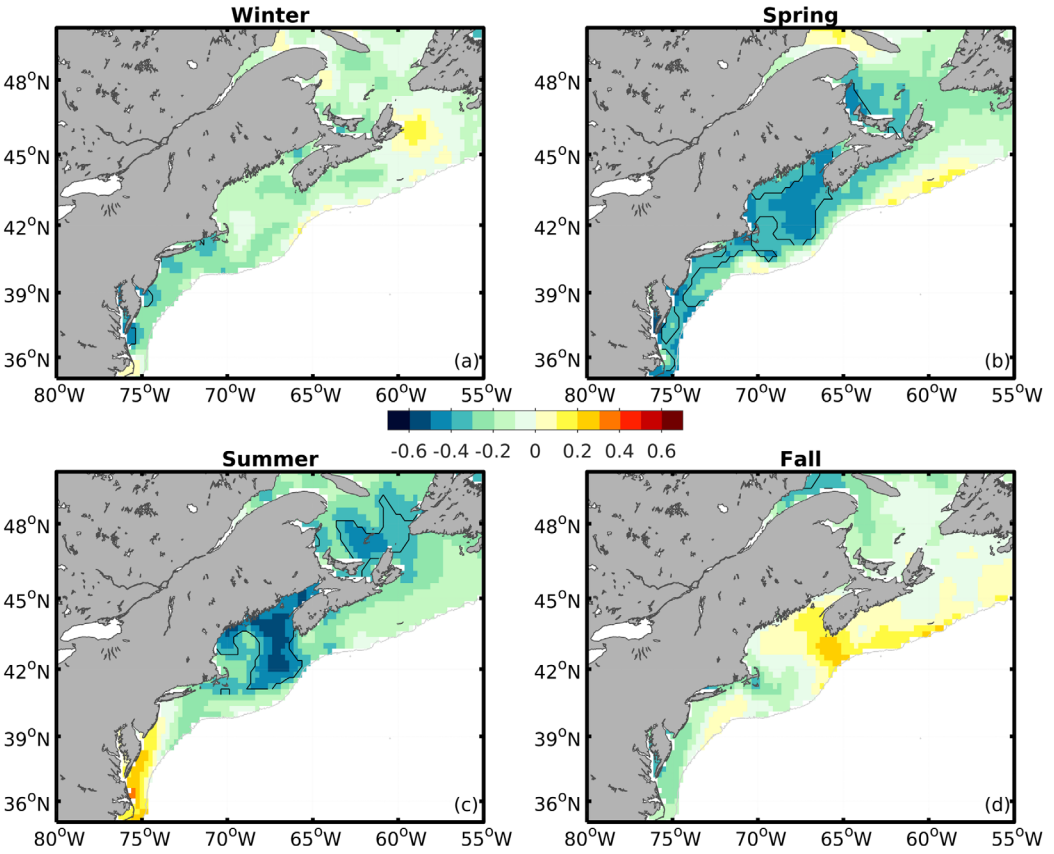

Figure 2. Interannual (1982–2014) linear correlation between Pacific Decadal Oscillation (PDO) index and sea surface temperature (SST) over the Northwest Atlantic in each season. The black contours denote the 95% significance level. Only results where the bathymetry is shallower than 1,000 m are shown. Linear trends are removed before the calculation of correlation. Degrees of freedom are calculated based on the integration of autocorrelation considering serial correlation (Emery & Thomson, 2001). The calculation of correlations in this work follows the same method.

are found in the spring and summer not only simultaneously but also with lags up to a few months. The maximum negative correlations are found with May–July/June–August GoM SST for a given spring/summer PDO. Therefore, the spring (April–June) PDO leads the GoM SST by 0–3 months (Figure 3, black circles),

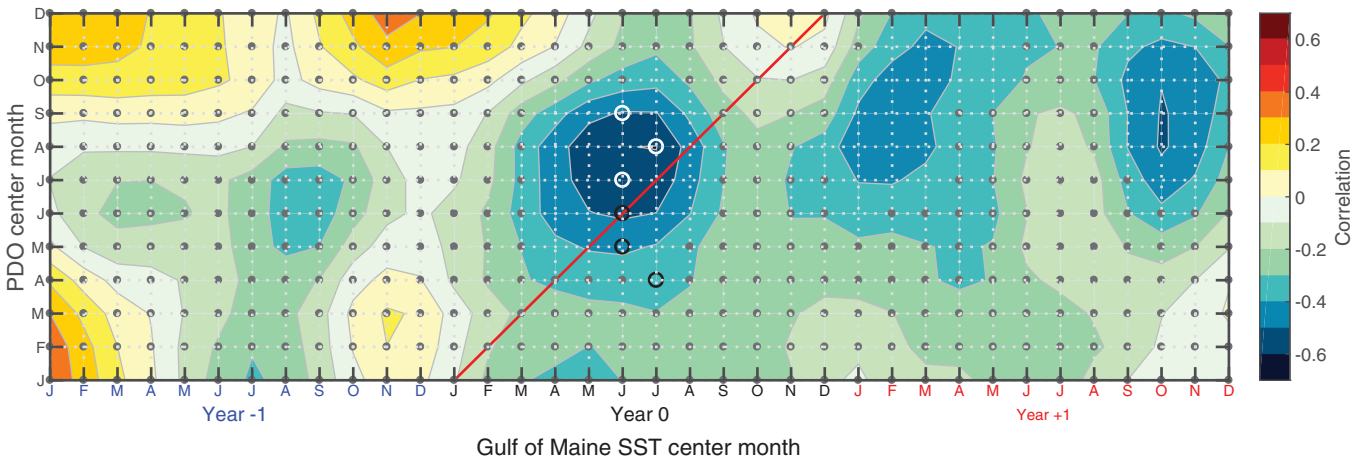

Figure 3. Lead-Lag correlation between 3 monthly PDO index and Gulf of Maine SST during 1982–2014. Both time series are linearly detrended. Dotted regions represent significance level lower than 95%. The red line denotes the concurrent correlation and thus PDO leads (lags) on the right (left) side of the line. The black (white) circles indicate the maximum correlation for the given spring (summer) PDO time series.

while the summer (July–September) PDO lags the GoM SST by about 1–3 months (Figure 3, white circles). The strongest cross correlation occurs when June–August GoM SST leads July–September PDO by 1 month, with the maximum correlation being $r = -0.60$, which is significant at 99% level. As we further discuss below in section 5 and 6, the fact that the maximum correlation was found when the GoM SST leads the summer PDO may not necessarily imply the GoM SST is physically driving the summer PDO. Over longer lead/lag scale, there are also other noticeable negative correlations when the PDO leads, but the correlations are less coherent and weaker. Repeating the analysis in Figures 2 and 3 using 10 year high-pass filtered PDO index produces very similar results (not shown), suggesting the interannual component of the PDO as the dominant source of the correlation.

The correlation analysis reveals that the relationship between PDO and Northwest Atlantic shelf SST has strong seasonal dependence. Spring and summer are the two seasons when PDO and SST have the strongest connection over interannual time scale. To understand this result, we need to examine the processes that are potentially associated with PDO and in the same time control the variability of the SST over the Northwest Atlantic shelf. As the correlation is between two variables from the two separated ocean basins, it is reasonable to speculate that oceanic processes are less likely the driving term. Instead, we start with atmospheric forcing terms of the upper ocean to search for the potential physical linkages.

3.2. Correlation Between PDO and Air-Sea Fluxes

The SST variability is controlled by the upper ocean mixed layer processes, which include the air-sea heat and momentum fluxes. To begin with, we examine the potential connection between the net air-sea heat flux (Q_{net}) and PDO, by calculating the linear correlation between PDO index and Q_{net} over the Northwest Atlantic continental shelf for each season during 1985–2009 (Figure 4), which is covered by all three heat flux products. Based on ERA-interim, Q_{net} (positive downward) in winter over most regions on the shelf including GoM are negatively correlated with the PDO index, although the correlations are not statistically

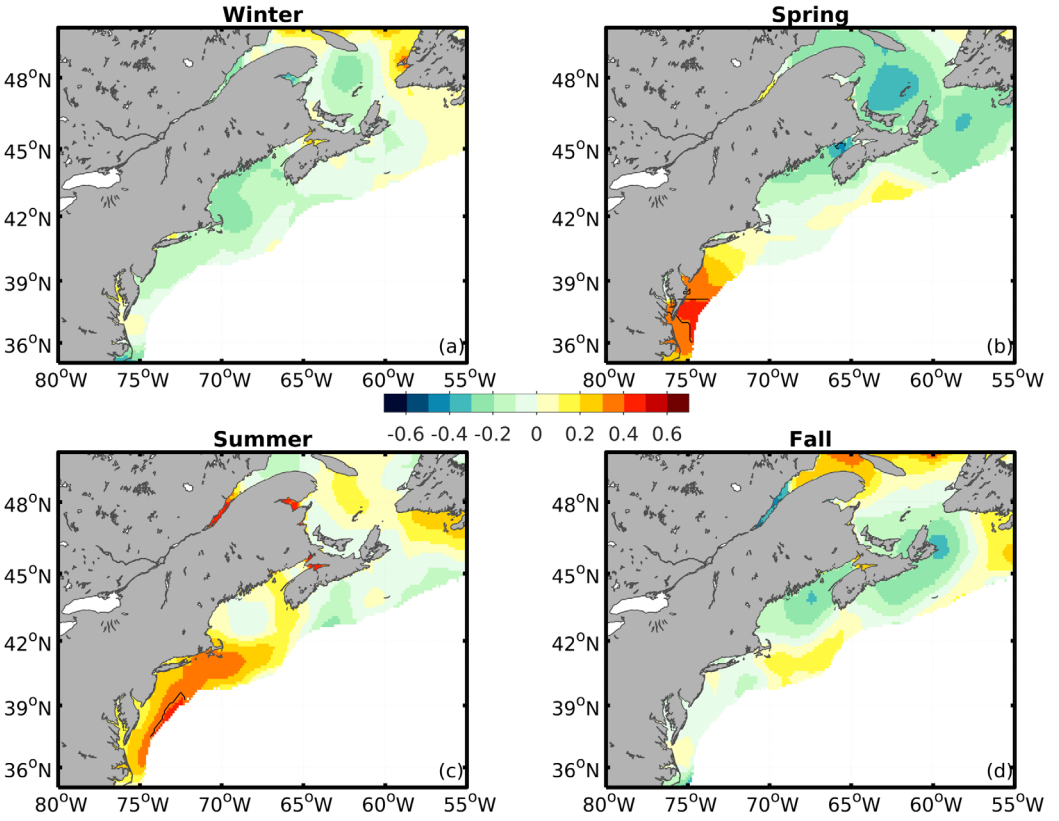

Figure 4. Same as Figure 2, but for interannual (1985–2009) linear correlation between PDO index and net air-sea flux (Q_{net}) over the Northwest Atlantic in each season. Technical details of the figures follow those in Figure 2. Data are derived from ECMWF ERA-Interim product.

Table 1
Interannual (1985–2009) Linear Correlations Between PDO Index and Air-Sea Surface Heat and Momentum Fluxes in the GoM (Polygon Defined in Figure 1)

		ERA-Interim	NARR	OAFlux
Spring	Q_{net}	−0.11	−0.23	−0.05
	SW	**−0.40**	**−0.49**	−0.28
	LW	**0.40**	**0.48**	0.23
	SH	0.04	−0.13	0.15
	LH	0.20	0.05	0.22
	WS	**0.43**	**0.46**	0.36
Summer	Q_{net}	0.16	0.01	−0.02
	SW	0.01	−0.35	0.03
	LW	0.09	0.34	0.31
	SH	0.05	0.03	0.16
	LH	0.16	0.20	0.18
	WS	−0.24	−0.05	−0.32

Note. Correlations significant above 95% confidence level are shown in bold.

significant. For spring, the negative correlations are more confined in the GoM, and northern regions in the Gulf of St. Lawrence and Laurentian Channel, with slightly more negative correlation. As shown in Figure 2c, GoM SST in summer is strongly correlated with PDO, but such a pattern is missing from the Q_{net} correlation (Figure 4c). In fall, negative correlations are found in the GoM and northern Scotian Shelf. Parallel analyses using Q_{net} from NARR and OAFlux give qualitatively similar results. Focusing only on spring and summer in the GoM, Q_{net} from NARR has stronger negative correlations with PDO in spring, and correlation close to zero in summer (Table 1). Q_{net} from OAFlux in both seasons have weak correlation with PDO, probably due to the coarse resolution (Table 1). Despite the differences in three products, Q_{net} in spring does have stronger negative correlation with PDO in comparison to that in summer. Furthermore, repeating the analysis in Figure 4 using 10 year high-pass filtered PDO index produces very similar results (not shown), which again suggest the interannual component of the PDO as the dominant source of the correlation.

To infer the processes contributing to such a correlation pattern, we further examined the corresponding correlation between PDO index and different components of heat fluxes in spring and summer (Figure 5). Short-wave radiation from ERA-interim in spring over GoM and Gulf of St. Lawrence is strongly correlated with PDO with negative correlation significant above 95% level. In summer, the correlation is only weakly positive over much of the shelf. Long-wave radiation is also strongly correlated with PDO, with significantly positive correlations in the GoM. Such a strong correlation is missing in summer. The negative and positive correlations in short and long-wave radiations in spring are likely associated with cloud cover, which has opposite effects on short and long-wave radiations. Turbulent heat fluxes do not present strong negative correlations with PDO in spring or summer, which excludes them to be the major contributors to the negative correlations in Q_{net} (Figure 6). Examinations of NAAR and OAFlux reveal similar results. In all three products, short-wave radiation is the major contributor to the negative correlations between Q_{net} and PDO in spring although the correlations are much stronger in ERA-interim (Figure 5a) and NARR than those in OAFlux (Table 1). Also, turbulent heat fluxes in all three products do not have significant correlations with PDO and thus are not the major contributors to the correlation.

In addition to heat flux, momentum flux can also significantly impact the upper ocean temperature by influencing the mixed layer depth via turbulent mixing. We examine the correlations between PDO and surface wind speed in spring and summer to search for potential connections. In all three products except OAFlux, wind speed in spring has significantly positive correlations in the GoM (Figure 6e and Table 1). In summer, the correlations are negative and weaker in all three products.

The above correlation analysis was also repeated using 10 year high-pass filtered PDO index. The results are very similar (not shown) and provide consistent information based on all three products. Over interannual time scale during 1985–2009, PDO is negatively correlated with Q_{net} over the GoM in spring, although the correlation is weak. Such a pattern is primarily the result of variability in radiative fluxes, which are strongly correlated with PDO. In comparison, the relationship between PDO and Q_{net} in summer is rather weak.

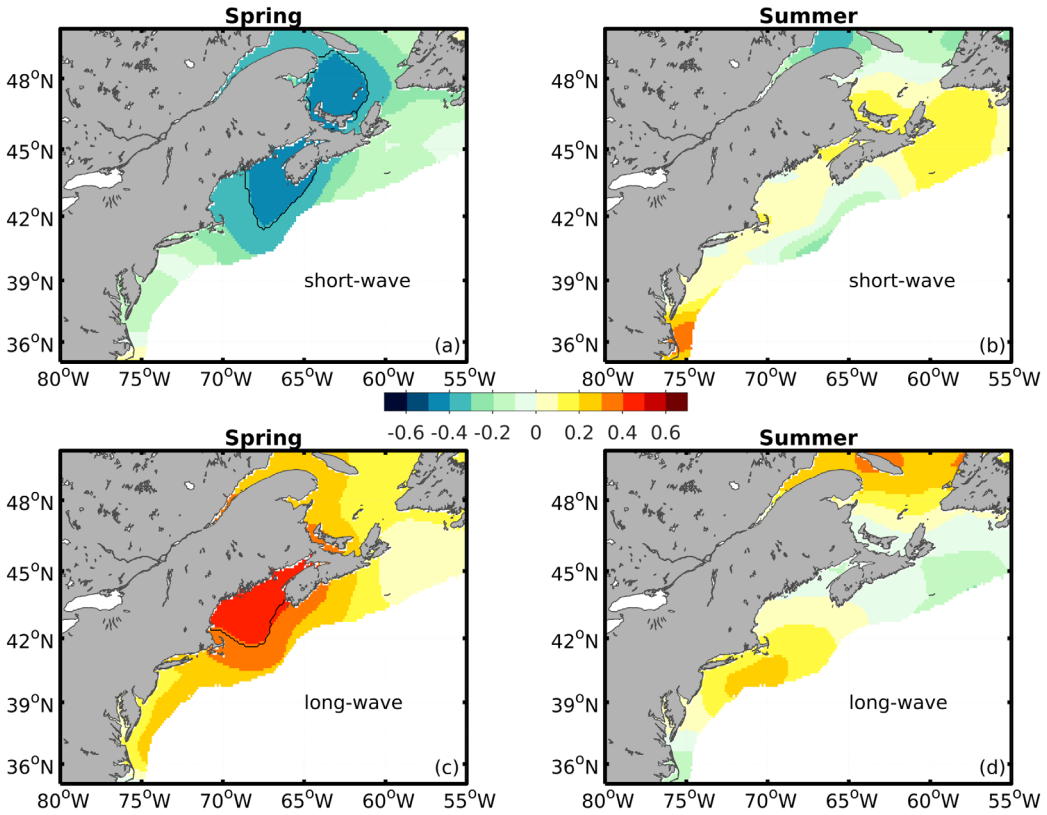

Figure 5. Interannual (1985–2009) linear correlation between PDO index and radiation heat fluxes (short-wave radiation in Figures 5a and 5b; long-wave radiation in Figures 5c and 5d) over the Northwest Atlantic in spring and summer. Technical details of the figures follow those in Figure 2. Data are derived from ECMWF ERA-Interim product.

Wind speed, which could be indicative of mixed layer depth, has significantly positive correlations with PDO in spring. This connection weakens in summer with non-significant negative correlations. The more robust correlations in spring lead to a plausible explanation of the strong negative correlation between PDO and SST in spring. Neglecting oceanic terms, integrating and averaging equation (2) over one season gives:

$$\overline{T} = T_0 + \overline{\int_{t_0}^{t_i} \frac{Q_{net} - q_{-h_m}}{\rho_0 C_p h_m} dt} \tag{3}$$

where $\bar{0}$ denotes seasonal mean, so $\overline{T}$ is the seasonal mean temperature, T_0 is the initial temperature at the beginning of the season, and $\overline{\int_{t_0}^{t_i} \frac{Q_{net} - q_{-h_m}}{\rho_0 C_p h_m} dt}$ is the mean cumulative heat flux over one season. Based on the correlation analysis for spring, a larger PDO index value corresponds to smaller Q_{net} and deeper h_m associated with stronger winds. The combination results in a smaller mean cumulative heat flux, which in turn could result in a colder seasonal mean temperature in spring. In other words, air-sea flux processes can explain the negative correlation between PDO and SST in the GoM in spring (Figure 2). In comparison, due to the weak correlations between PDO and Q_{net}/wind, the strong negative correlations between PDO and SST in summer can less likely be explained by the atmospheric forcings. Instead, it is reasonable to hypothesize that the relationship between PDO and SST in summer is more contributed by oceanic processes, which may rectify the atmospherically driven PDO to GoM SST connection in spring.

4. Mixed Layer Temperature Diagnosis

The plausible mechanism behind the negative correlation between PDO and GoM SST in spring and summer needs to be confirmed in a quantitative way. Specifically, we want to know whether air-sea flux and

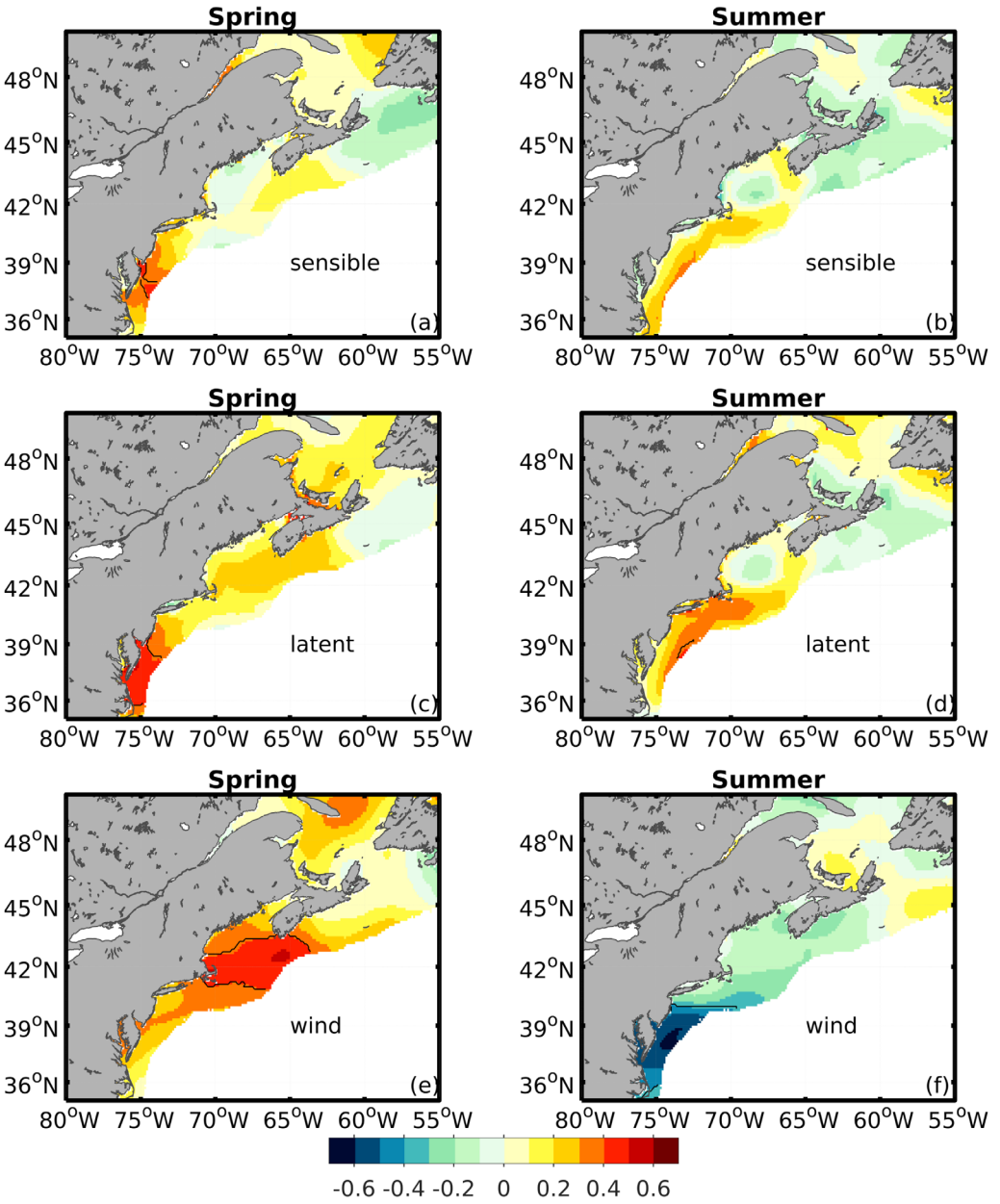

Figure 6. Same as Figure 5 but for turbulent heat fluxes (sensible heat flux in Figures 6a and 6b; latent heat flux in Figures 6c and 6d) and wind speed (Figures 6e and 6f). Technical details of the figures follow those in Figure 2. Data are derived from ECMWF ERA-Interim product.

upper mixed layer variability can explain the interannual SST variability in spring. We also hope to confirm that interannual SST variability in summer is more controlled by oceanic process e.g., horizontal advection. To do that, we reconstruct the multiyear, seasonal mean SST over the Northwest Atlantic continental shelf using (3), i.e., surface heat flux forcings only. Although the absence of shelf-wide observations prevents us from accurately calculating horizontal advective flux $\mathbf{u}_m \cdot \nabla T_m$ or vertical entrainment $\frac{w_e \Delta T}{h_m}$, a diagnostic calculation using atmospheric forcing only could shed light on the relative importance of atmosphere and ocean in determining the interannual variability of SST in each season. This can further inform us about the potential mechanism underlying the PDO-SST correlation.

We initialize the PWP model 1 month before the starting month of the season and integrate 4 months to cover the full season. For comparison purpose, we choose 1989–2009 as the analysis period, which is covered in all data sets (CCMP vector wind data are only available from 1989, and OAFlux terminates in 2009).

This gives daily temperature and salinity profiles at each grid point from 1989 to 2009. As the initial profile is monthly climatology, starting 1 month before the season with realistic atmospheric forcings provides the model spin-up adjustment. To reconstruct the seasonal mean temperature, we extract from the observations the initial temperature at the beginning of the season for T_0, realistic net air-sea flux for Q_{net}, and penetrating short-wave radiation at the base of the mixed layer for q_{-h_m}. Furthermore, based on the PWP model output, we define the mixed layer depth h_m to be the upper-ocean layer whose depth-averaged temperature is 0.5°C higher than the water temperature just below it:

$$\Delta T = T_m - T_b \equiv \frac{1}{h}\int_{-h_m}^{0} T(z)dz - T_b = 0.5^{\circ}C \tag{4}$$

where T_b is the water temperature just below the mixed layer. This definition follows Qiu and Kelly (1993) but uses 0.5°C as the criterion as opposed to 1°C. Based on sensitivity experiments, the difference in this value (including 1°C) or using another temperature gradient criterion (Monterey & Levitus,) do not impact the major results below.

The comparison between our reconstructed SST and the AVHRR OI SST for spring and summer in the GoM (polygon enclosed by the dashed line and the coastline in Figure 1) unravels the different operating processes in different seasons. The reconstruction in spring based on equation (3) compares favorably well with the observation-based SST in terms of both interannual variability and magnitude (Figure 7a). Linear correlation between the two is 0.75, significant at 99% confidence level, and Root-Mean-Square Difference (RMSD) is 0.75°C. In comparison, the reconstructed SST in summer fails to capture the interannual variability

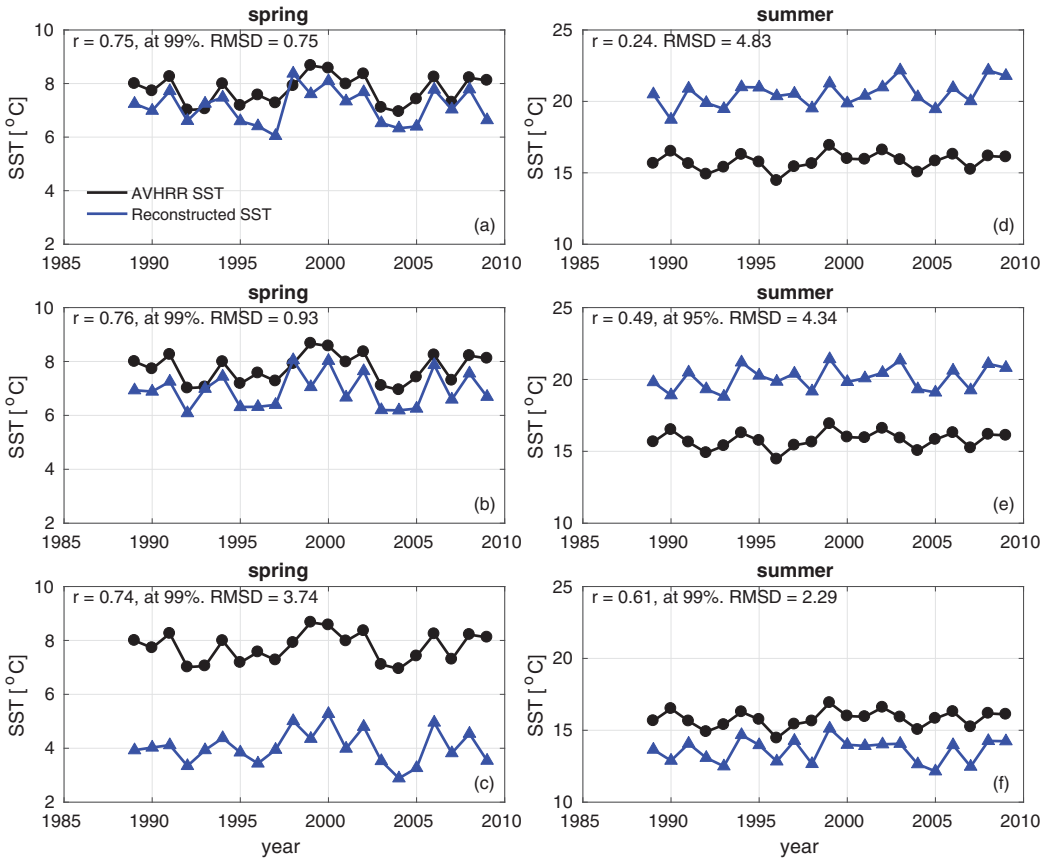

Figure 7. Comparisons of AVHRR SST (black) and reconstructed SST (blue) for (left column) spring and (right column) summer in the GoM (delineated in Figure 1). Figures 7a and 7d: Reconstructed SST using the combination of initial temperature and time-varying air-sea heat flux as well as time-varying mixed layer depth. Figures 7b and 7e: Reconstructed SST as in Figures 7a and 7d, but using constant climatological seasonal mean mixed layer depth instead. Figures 7c and 7f: Initial temperature only. In each figure, linear correlation with statistical significance level and root mean square difference (RMSD) are shown.

and overestimates the average magnitude from year to year (Figure 7d). Linear correlation is only 0.24, not even reaching 90% confidence level, and the RMSD is 4.8°C. The results suggest that interannual SST variability in spring can be largely explained by the local 1-dimensional mixed layer processes (the combination of initial temperature and heat flux accounts for the interannual variability in spring). However, summer SST variability is more controlled by oceanic processes, e.g., along-shelf advection (the combination of initial temperature and ocean advective flux accounts for the interannual variability in summer).

To understand the contributions of each term in equation (3), we also reconstruct SST using climatological mean constant h_m (over the analysis period) and thus eliminated the effect of mixed layer depth variability. For spring, the interannual variability of such reconstructed SST in the GoM still compares well with the AVHRR OI SST counterpart, but the difference in magnitudes increase (Figure 7b). Dropping the entire surface flux term $\overline{\int_{t_0}^{t_i} \frac{Q_{net}-q_{-h_m}}{\rho_0 C_p h_m} dt}$, the reconstructed SST using only the initial temperature of the season still results in comparable correlation (0.74) but underestimated magnitude (Figure 7c).

For summer, reconstruction using climatological h_m (Figure 7e) yields a better correlation with observation-based SST than that of reconstructed SST using interannually varying h_m (Figure 7d). At a first glance, this might seem surprising as it indicates moving away from being realistic produces a better result. However, comparing initial temperature of the season and seasonal mean temperature, we see a significant correlation (0.61, at 99% confidence level), and a better estimate of magnitude (Figure 7f). In other words, adding the surface heat flux forcing terms $\overline{\int_{t_0}^{t_i} \frac{Q_{net}-q_{-h_m}}{\rho_0 C_p h_m} dt}$ to the seasonal mean temperature budget in summer without considering oceanic processes actually degrades the estimation in that the reconstructions increased the already overestimated magnitude and worsened the reproduction of the year-to-year variability. This is contrasting with the spring case, in which considering the surface heat flux forcing with realistic mixed layer variability improves the estimation of seasonal mean temperature. Repeating the different reconstruction scenarios using NARR and OAFlux gives similar results (Figures A1 and A3). In both sets of results, considering surface heat flux forcing yields a better reconstruction in spring, and adding surface heat flux forcing to the initial temperature in summer actually degrades the reconstruction. The correction from Figures 7c to 7b and then to Figure 7a is primarily due to the role of the climatological mean surface heat fluxes. Combined with the summer figures, this analysis supports the idea that the climatological SST in the GoM is primarily driven by surface heating in the spring and advective cooling in the summer. Furthermore, the role of time-varying surface heat flux and mixed layer depth in the interannual variability of the GoM SST is shown by considering the correlations between the PDO and various reconstructed GoM SST (Figure 8). Only the reconstruction using the interannual varying heat flux and mixed layer depth in spring reproduced the significant negative correlation (Figure 8a).

The degraded reconstruction in summer indicates the missing oceanic processes are important in modulating the summer temperatures on the Northwest Atlantic shelf from year to year. This is probably associated with ocean advective cooling since the reconstructed SST is higher than the observed SST in summer (Figure 7d). If we assume the along-shelf advection is the dominant term in the missing oceanic processes, i.e., neglecting the cross-shelf advection and vertical entrainment, we can infer the magnitude of the mean cumulative along-shelf advective flux over 3 months $\overline{\int u_m \frac{\partial T_m}{\partial x} dt}$, which ranges between -6.2 and -2.2°C based on the difference between the observed and reconstructed SST in the Figure 7d. Continuing the back-of-the-envelope calculation, we take the two cross-shelf transects encompassing the GoM (Figure 1) and consider the differences in transect-averaged temperature, and the distance along the 1,000 m isobath to calculate the along-shelf SST gradient (not shown). If we assume a constant along-shelf velocity over 3 months, $\overline{\int u_m \frac{\partial T_m}{\partial x} dt} \approx u_m \overline{\int \frac{\partial T_m}{\partial x} dt}$, then we can infer the along-shelf current across the GoM within the mixed layer to be 0.06 to 0.18 m/s. These numbers are comparable to the long-term mean depth-averaged along-shelf current in the Middle Atlantic Bight of 0.03 to 0.1 m/s (Lentz, 2008) and the more energetic, surface-intensified shelfbreak jet velocity of ~0.2–0.4 m/s at Southern New England Shelf (Chen & He, 2010; Fratantoni et al., 2001; Linder & Gawarkiewicz, 1998). Despite the simplified calculations, ocean advective flux being the dominant term in determining the summer SST in the Northwest Atlantic coastal ocean is reasonable.

We can further evaluate the different reconstructions by correlating the reconstructed SST with the PDO index in spring and summer, and compare the correlations with those based on observations in terms of the spatial pattern. For spring, reconstructed SST based on surface heat flux forcing and realistic mixed layer

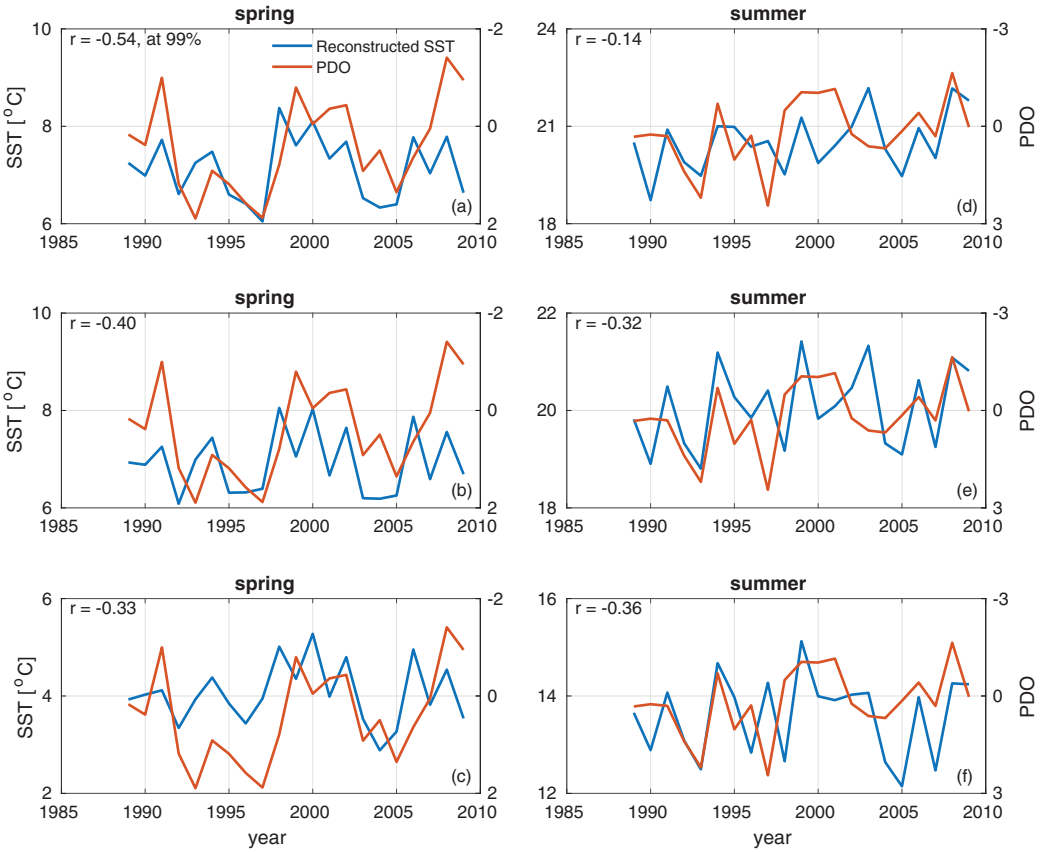

Figure 8. Same as Figure 7 but for PDO index (red, right axes) and reconstructed SST (blue, left axes) for (left column) spring and (right column) summer in the GoM (delineated in Figure 1). Note the PDO axes are flipped for better visual comparison.

variability successfully reproduces the statistically significant negative correlations in the GoM (compare Figure 9b with Figure 9a). There are differences in the spatial structure and the magnitude, but it is encouraging to see the skills of such a reconstruction based on simple considerations of the local 1-dimensional process. This is particularly true in comparison to the correlations of the reconstructed SST in summer. Apparently, the reconstruction fails to capture the strong negative correlation between PDO and SST in the GoM in summer (Figure 9f). Strong correlations are located outside of the GoM, different from the results in Figure 9e. Furthermore, consideration of $\overline{\int_{t_0}^{t_i} \frac{Q_{net}-q_{-h_m}}{\rho_0 C_p h_m} dt}$ in spring significantly improves the reconstruction over the other two cases (Figures 9c and 9d). This is not the case in summer as the inclusion of $\overline{\int_{t_0}^{t_i} \frac{Q_{net}-q_{-h_m}}{\rho_0 C_p h_m} dt}$ results in weaker correlations with PDO, which again indicates oceanic processes are important in summer. Parallel calculations using NARR and OAFlux reach very similar conclusions (Figures A2 and A4).

5. Atmospheric Bridge From the Pacific to Gulf of Maine

In spring, the changes in Pacific are likely impacting the GoM SST via the atmospheric teleconnection. The correlation patterns of April–June global SST, sea-level pressure (SLP), and 500 hPa geopotential height (Z500) anomalies against the GoM SST in spring (May–July) further provide evidence on the potential atmospheric bridge from the North Pacific to the GoM (Figure 10). It is worth noting that the spring SST anomalies in the North Pacific associated with the GoM SST variability is not exactly the canonical PDO spatial pattern (as the eastern tropical Pacific and the Kuroshio extension exhibit the anomalies of the same sign) but more similar to the so-called the ENSO precursor pattern (Vimont, 2005) with greater amplitudes in the central and eastern North Pacific. Therefore, the PDO may not properly represent springtime Pacific forcing on GoM SST, despite

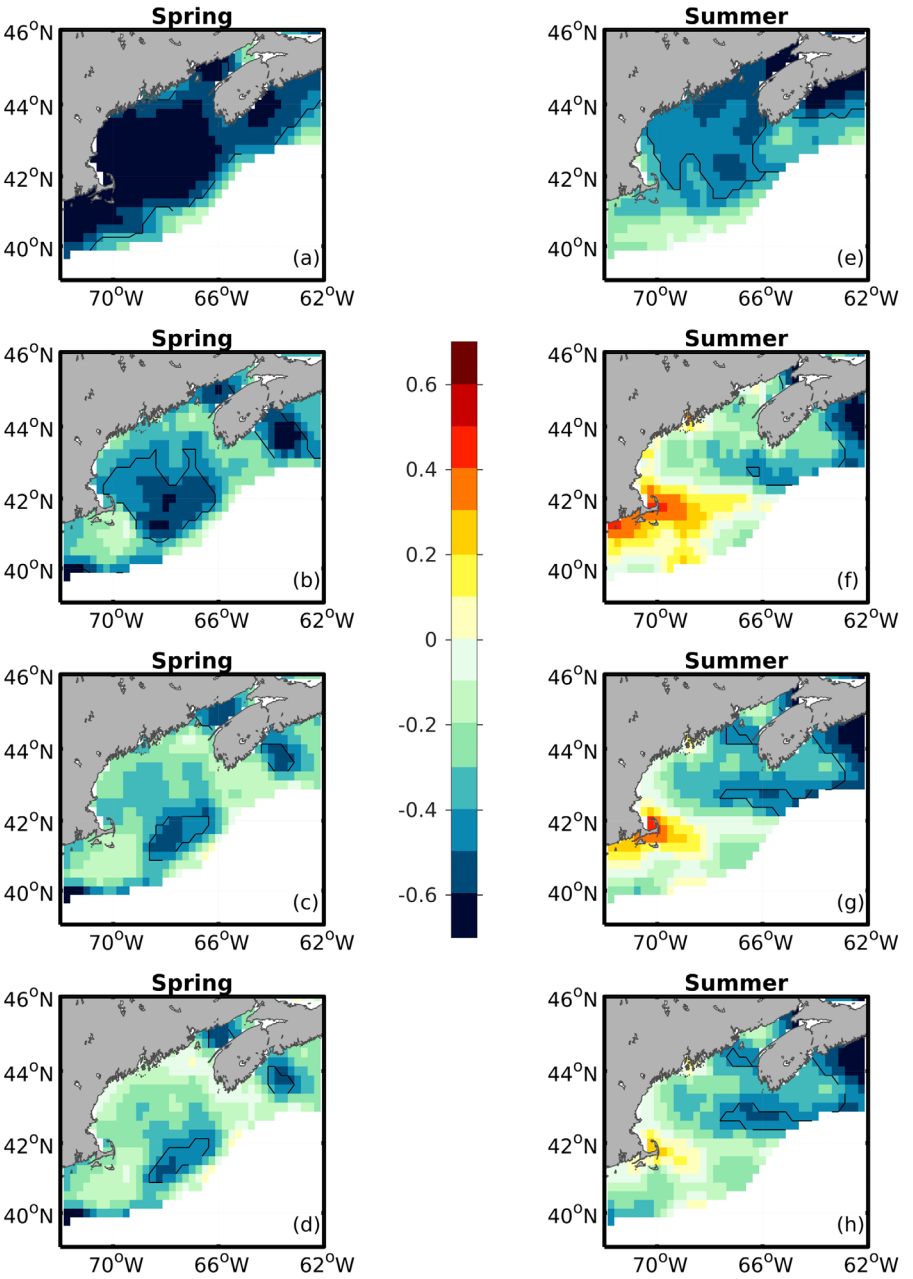

Figure 9. Interannual (1989–2009) linear correlation between PDO index and reconstructed SST over the Northwest Atlantic in spring and summer. Figures 9a and 9d: OISST for comparison purpose. Figures 9b and 9f: Reconstructed SST using the combination of initial temperature and time-varying air-sea heat flux as well as time-varying mixed layer depth. Figures 9c and 9g: Reconstructed SST as in Figures 9a and 9d, but using constant climatological seasonal mean mixed layer depth instead. Figures 9d and 9h: Initial temperature only. Technical details of the figures follow those in Figure 2.

the high correlation. We also checked the results in the South Pacific (not shown), and found that the high correlations are mostly in the North Pacific. The correlations in the South Pacific are weak and insignificant.

By focusing on the SST anomalies in the central North Pacific (155°–180°W, 25°–40°N) instead of the basin-wide PDO, we can show more clearly that the central North Pacific SST anomalies leading the GoM SST (Figure 11a). More importantly, the outgoing long-wave radiation (which is a proxy for the tall cloud amount) anomalies in the eastern North Pacific (135°–155°W, 25°–40°N) leads the spring GoM SST by a couple of months (Figure 11b). This result can be reproduced by using precipitation averaged over the same region instead of the outgoing long-wave radiation (not shown). On the other hand, the precipitation and

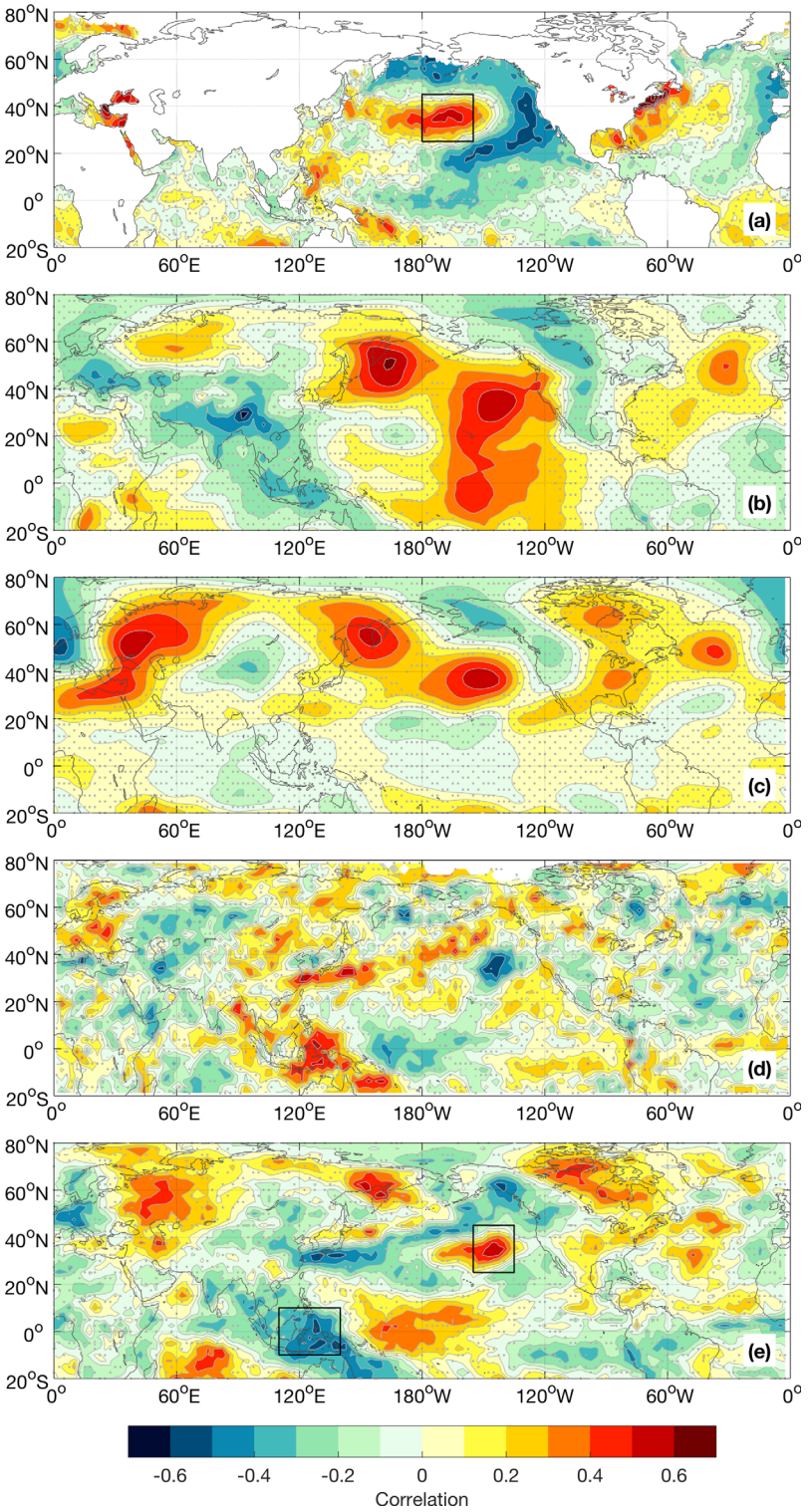

Figure 10. Correlation of the global April–June (a) SST, (b) sea-level pressure, (c) 500 hPa geopotential height, (d) precipitation, and (e) outgoing long-wave radiation against the SST averaged in the Gulf of Maine in May–July, 1982–2014. Dotted area denotes significance level lower than 95%. Data are monthly means from the Hadley Centre Sea Ice and Sea Surface Temperature data set (HadISST v1), NCEP/NCAR (National Centers for Environmental Prediction/National Center for Atmospheric Research) Reanalysis 1, NOAA Climate Prediction Center (CPC) Merged Analysis of Precipitation (CMAP), and NOAA CPC Interpolated Outgoing Long-wave Radiation, respectively. The black rectangular boxes in Figures 10a and 10e are the average region used in the Figure 11.

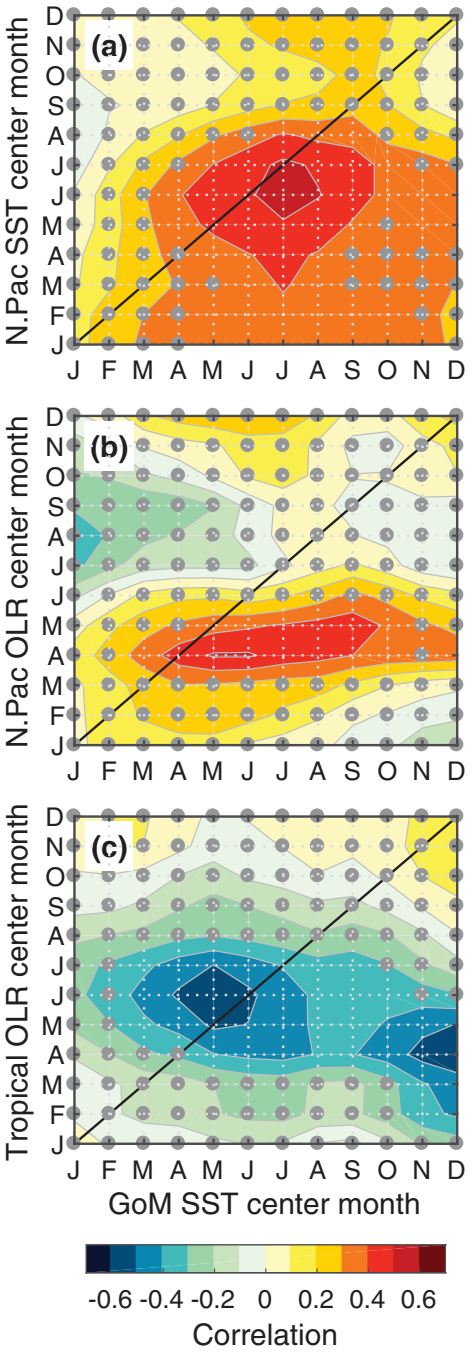

Figure 11. Lead-Lag correlation of 3 monthly (a) SST in the North Pacific (155°–180°W, 25°–40°N), (b) outgoing long-wave radiation (OLR) in the North Pacific (135°–155°W, 25°–40°N), and (c) OLR in the tropical Indo-Pacific (110°–140°E, 10°S–10°N) against Gulf of Maine SST during 1982–2014. The averaging regions are indicated in the Figure 10. All the time series are linearly detrended. Dotted regions represent significance level lower than 95%. The black diagonal lines denote the concurrent correlation and thus Gulf of Maine SST leads (lags) on the left (right) side of the line.

outgoing long-wave radiation over the maritime continent (110°–140°E, 10°S–10°N) lags the spring GoM SST similarly to the PDO (Figure 11c).

The Pacific-North American pattern (PNA; Wallace & Gutzler, 1981)-like teleconnection in SLP and Z500 anomalies (with an equivalent barotropic vertical structure) are propagating out from the central/eastern North Pacific, although it is not entirely clear whether the SST anomalies are driving the teleconnection or the other way around. The central/eastern North Pacific being the center of action for affecting the downstream variability over the North America and North Atlantic is consistent with the recent seasonal predictability study by McKinnon et al. (2016). In addition, Dai et al. (2017) recently showed that a flavor of the PNA teleconnection, which are not driven by the tropical convection, experience rapid growth in the central/eastern North Pacific through barotropic wave amplification.

However, it is still unclear how this atmospheric teleconnection from central/eastern North Pacific is affecting the cloud cover and the radiative heat flux over the Gulf of Maine. Perhaps one possibility is that the anticyclonic SLP anomalies over the Northwest Atlantic (Figure 10b) may enhance the southerly advection of moistures from the Gulf of Mexico into the Gulf of Maine to increase the cloud cover. The Gulf of Mexico has been shown to be the primary source of the moisture along the east coast of U.S. and Northwest Atlantic, especially through the synoptic and intraseasonal eddy fluxes (Kwon & Joyce, 2013; Newman et al., 2012). In particular, the intraseasonal variability such as blocking high pressure anomalies and associated jet stream variability are shown to have significant impact on the regional climate (Chen et al., 2014; Santos et al., 2013).

6. Discussions and Summary

In this work, we examine the relationship between the basin-scale Pacific variability represented by Pacific Decadal Oscillation (PDO) and sea surface temperature (SST) in the Northwest Atlantic coastal ocean over interannual time scale. Consistent with the previous findings by Pershing et al. (2015), statistically significant negative correlations were found in spring and summer, particularly in the Gulf of Maine (GoM). Cross-correlation analysis between the PDO and GoM SST further suggests a significantly negative lead-lag correlation, with the spring PDO leading the GoM SST by 0–3 months while the summer PDO lagging by 1–3 months. The correlations are dominated by the interannual variability. These results suggest a connection lasting over seasonal scale within the system.

n spring, the changes in the North Pacific are likely to impact the GoM SST via a PNA-like atmospheric teleconnection. The spring SST, precipitation, and outgoing long-wave radiation anomalies in the central and eastern North Pacific are shown to lead the GOM SST by 1–3 months. While the PNA-like teleconnection in SLP and 500 hPa geopotential height seem to originate from the central/eastern North Pacific, it is not clear whether the teleconnection is driven by local heating anomalies or just experiencing a rapid growth there. Nevertheless, the central/eastern North Pacific being an important region for the atmospheric planetary wave propagation downstream over the North America and North

Atlantic is consistent with other recent studies (Dai et al., 2017; McKinnon et al., 2016). A general circulation model-based future investigation would be useful to clarify the teleconnection mechanism.

Regardless of the uncertainties in the atmospheric bridge that operates between North Pacific and Northwest Atlantic and its impact on the radiative fluxes over the Gulf of Maine, the contributions from the surface heat flux and oceanic forcings on the upper ocean mixed layer temperature are more conclusive. In spring, the radiation fluxes dominated the interannual variability of net air-sea heat flux, which together with the varying mixed layer depth potentially modulated by the wind largely controls the temperature variability from year to year. Chen et al. (2016) also showed that the interannual variability of winter-spring depth-averaged temperature in the Middle Atlantic Bight is primarily controlled by air-sea heat flux. Despite the different targets, i.e., depth-averaged temperature versus SST, current analysis is consistent with Chen et al. (2016) in that atmospheric forcing plays a dominant role in modulating year-to-year spring temperature over the Northwest Atlantic shelf.

In contrast, summer SST variability over interannual time scale cannot be explained by surface heat flux forcings. Instead, ocean advective cooling is likely the primary mechanism determining the temperature variability. We further confirm the diagnosis of atmospheric and oceanic processes in controlling the upper mixed layer temperature by examining the spatial distribution of the correlation between PDO and reconstructed SST. Considering only 1-D mixed layer processes, the reconstructed SST in spring generally reproduces the spatial correlation pattern in spring. However, the same consideration does not apply for summer temperature variability. We have examined the above mixed layer diagnosis using three different products including ERA-interim, NARR, and OAFlux, and reached the same conclusions.

In summary, our results suggest the Pacific variability influences the GoM SST primarily in spring through the atmospheric teleconnection. Then, the remaining puzzle is why we obtain a greater correlation for the summer PDO with the GoM SST leading by 1–3 months. We do not find any evidence for the GoM SST impacting the summer PDO. Therefore, our results may suggest that the significant interannual correlation between PDO and GoM SST in summer, with the PDO lagging by 1–3 months, is perhaps a convoluted result from the long decorrelation time scale of PDO and GoM SST, respectively, in addition to the seasonal evolution of the SST anomaly pattern in the Pacific. The GoM SST anomalies exhibit a very strong persistent pattern particularly from spring to summer (Figure 12). PDO also has relatively long decorrelation scale (Newman et al., 2016), with the correlation between the spring and summer PDO being $r = 0.6–0.7$ (not shown). Perhaps a more important factor is that the spring Pacific SST anomaly pattern associated with the GoM SST is not exactly the PDO pattern as already pointed out (Figure 10). Therefore, the PDO index may not be the most appropriate index to be used to study the relationship between the Pacific variability and GoM SST, although it is the most popular and convenient index. Furthermore,

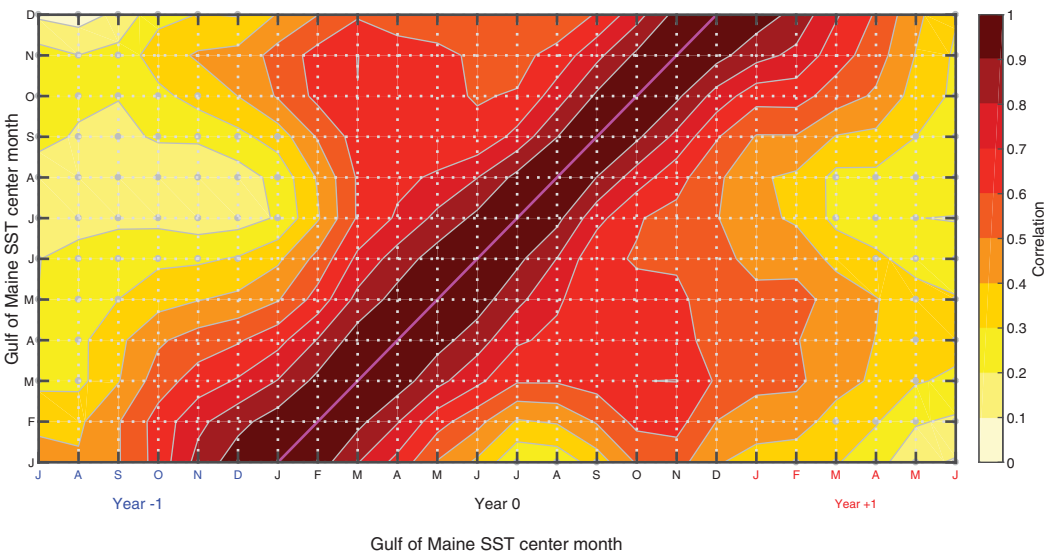

Figure 12. Autocorrelation of GoM SST (AVHRR) based on detrended 3 month running mean from 1982 to 2014. Dotted area denotes significance level lower than 95%.

the PDO is not a single physical mode of variability, but an empirical mode that may include at least three distinct physical modes (Newman et al., 2016). It is possible that the spring Pacific SST anomaly pattern evolve in a few months into a pattern that projects better to the PDO pattern, without further impacting the GoM SST. However, we cannot fully exclude the possibility for the correlation between the spring GoM SST and summer PDO actually reflecting the connection from Atlantic to Pacific, although the GoM SST may not be the primary driver. For example, some climate modeling studies suggested that the Atlantic multidecadal variability, the leading mode of the North Atlantic SST variability, can drive PDO-like pattern in the Pacific (Ruprich-Robert et al., 2017).

The other result that is worth noting is the nonstationary relationship between PDO and GoM SST. Correlations were calculated for the period of 1982–2014 in current analysis and 1982–2013 in Pershing et al. (2015). The PDO index and GoM SST in spring and summer are significantly correlated. We have repeated the same correlation analysis using HadISST for the period of 1950–2014. However, no significant correlations were found in any season. This result reveals the changing relationship between the North Pacific variability and SST on the NW Atlantic continental shelf over a longer-time scale. Indeed, further examination using a 30 year moving correlation since 1900 reveals that the significant correlations in spring and summer are more pronounced in the recent period since late 1970s, although there are some significant correlations in other seasons in 1920–1950s (not shown). The examination of the changing connections over decadal scale and longer is beyond the scope of this work, though intriguing. Furthermore, it is not clear how much the data quality prior to the satellite SST period (1982-) affects the nonstationary relationship. The analysis here on interannual time scale should then be interpreted with the recent time period (1982–2014) in mind.

Our analysis highlights the complexity of the atmosphere-ocean system and the uncertainties in identifying mechanistic linkages within the system. While the importance of atmospheric forcing on SST has been identified, more work is needed to better elucidate the atmospheric pathway operating between the North

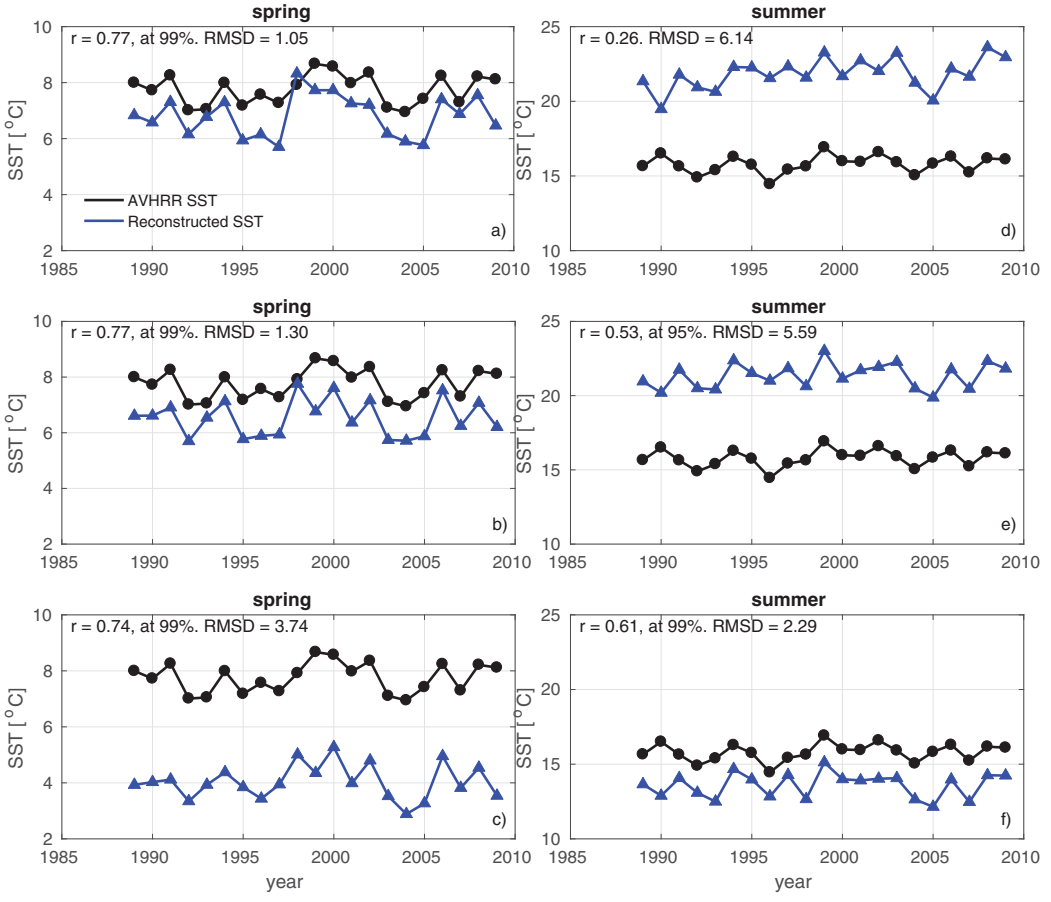

Figure A1. Same as Figure 7 but based on NARR.

Pacific and Northwest Atlantic. This is particularly important within the context of rapid changes in the global climate system and in the Northwest Atlantic coastal ocean.

Appendix

We cross-validate the key results using different sets of datasets. Figures A1 and A3 can be directly compared with Figure 7; Figures A2 and A4 can be directly compared with Figure 9.

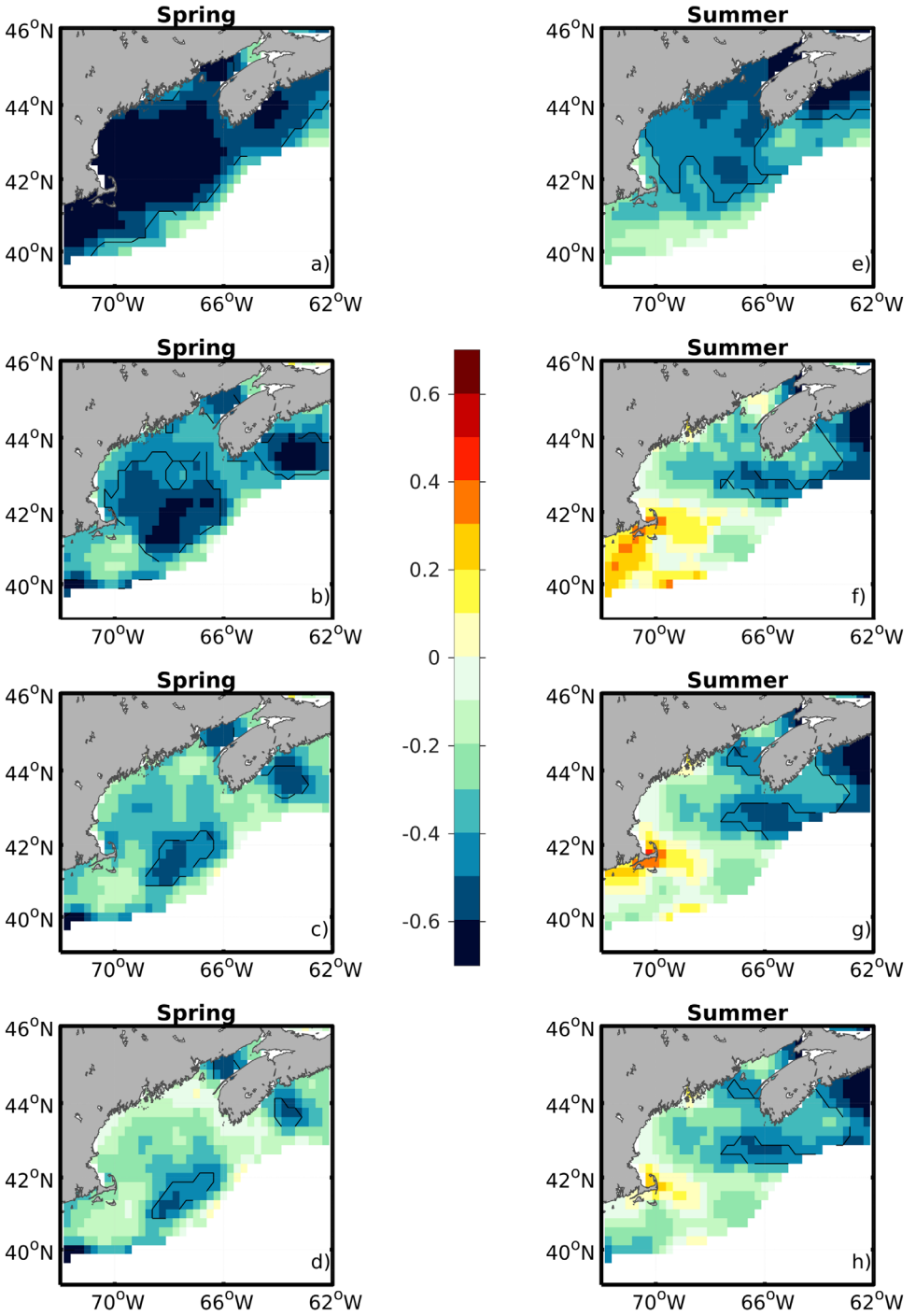

Figure A2. Same as Figure 9 but based on NARR.

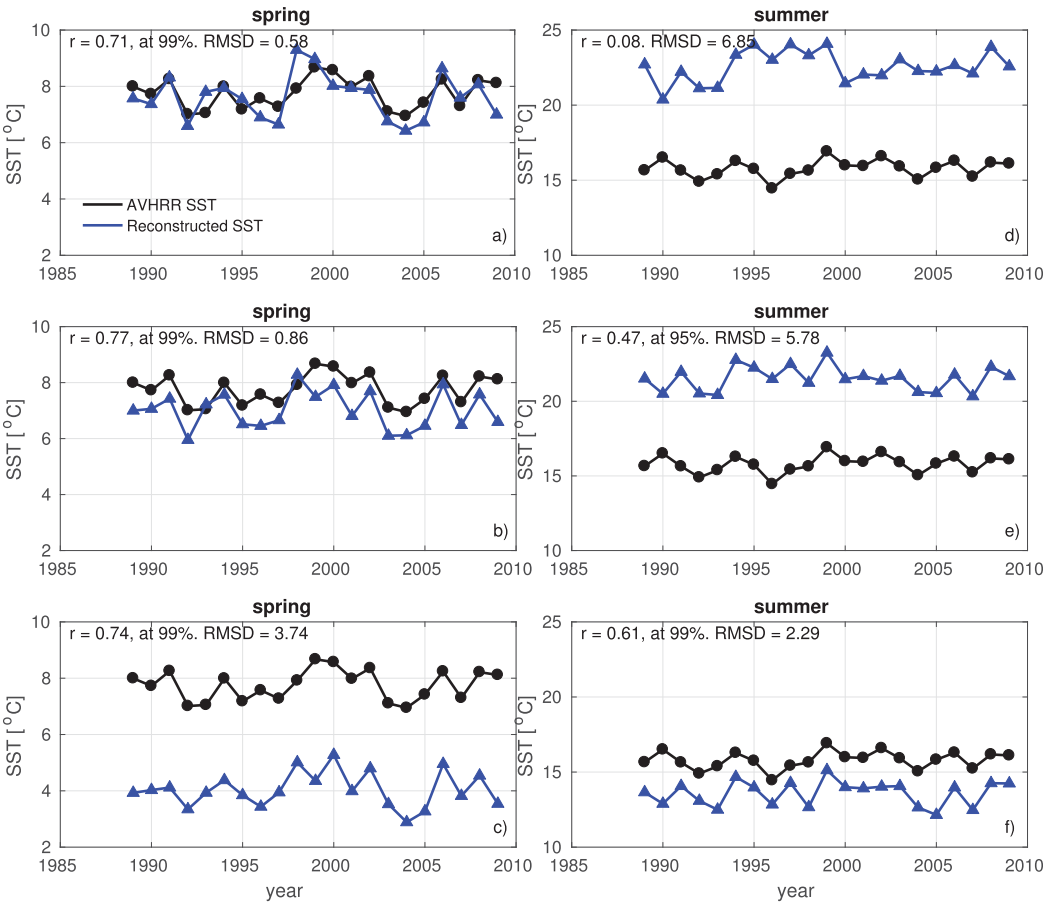

Figure A3. Same Figure 7 but based on OAFlux.

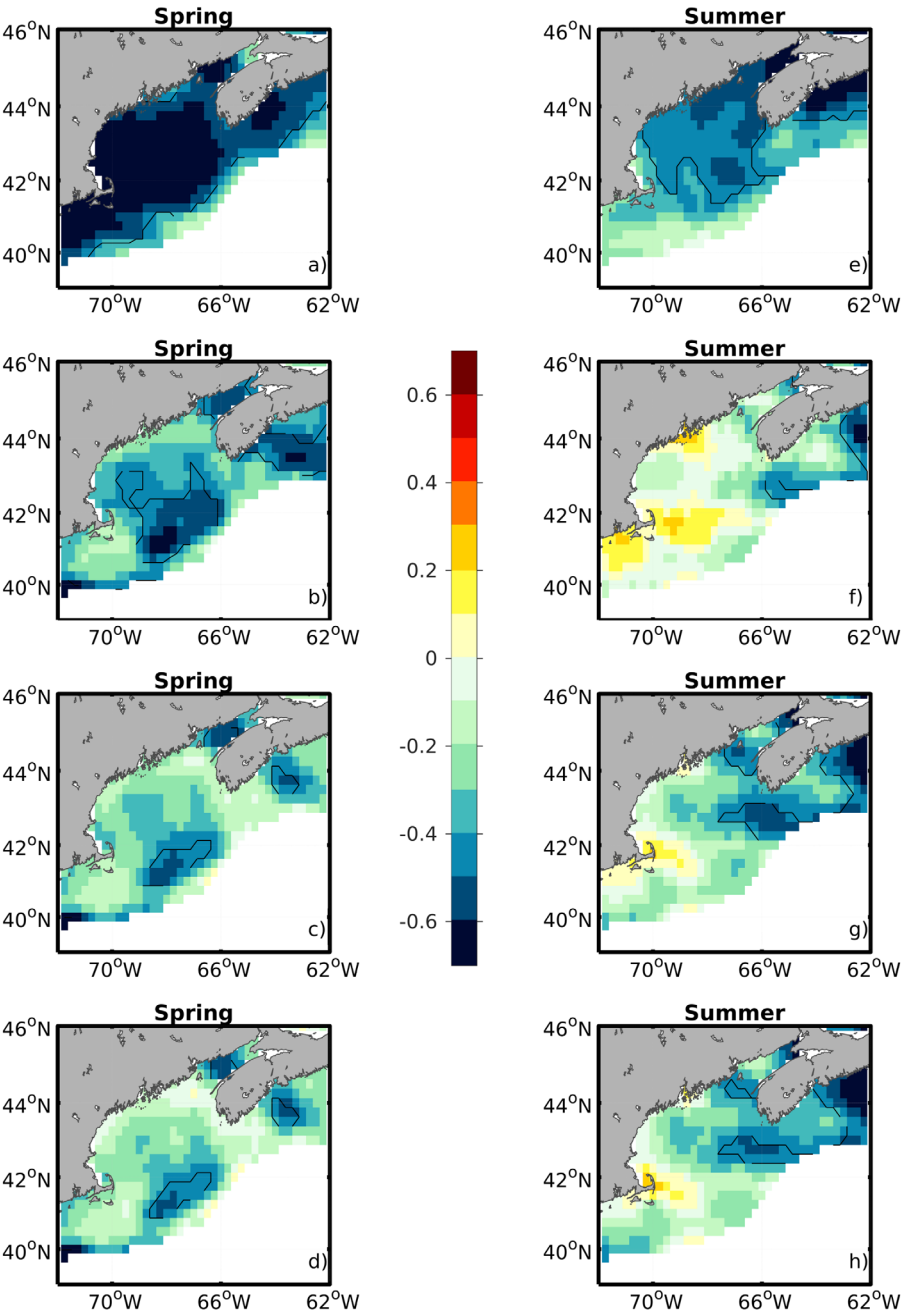

Figure A4. Same as Figure 9 but based on OAFlux.

Acknowledgement
This work was supported by the National Science Foundation Ocean Science Division with grant OCE-1435602 (K.C. and Y.-O.K.), OCE-1558960 (K.C.), and OCE-1634094 (K.C.), and National Oceanic and Atmospheric Administration Climate Program Office MAPP program with grant NA170AR4310111 (Y.-O.K. and K.C.). There is no new data or model used in this study. All the data are obtained from the publicly available data center web pages, which are specified in section 2.2. The original PWP model code is distributed by Jim Price at: http://www.whoi.edu/science/PO/people/jprice/PWP/pwp.f. A MATLAB version of the model is distributed by Peter Lazarevich and Scott Stoermer at: http://www.po.gso.uri.edu/rafos/research/pwp/.

References

Bane, J. M., Spitz, Y. H., Letelier, R. M., & Peterson, W. T. (2007). Jet stream intraseasonal oscillations drive dominant ecosystem variations in Oregon's summertime coastal upwelling system. *Proceedings of the National Academy of Sciences of the United States of America*, *104*, 13262–13267.

Barth, J. A., Menge, B. A., Lubchenco, J., Chan, F., Bane, J. M., Kirincich, et al. (2007). Delayed upwelling alters nearshore coastal ocean ecosystems in the northern California current. *Proceedings of the National Academy of Sciences of the United States of America*, *104*, 3719–3724.

Berrisford, P., Dee, D., Poli, P., Brugge, R., Fielding, K., Fuentes, M., et al. (2011). The ERA-interim archive version 2.0, ERA report series (Vol. 1). Reading, UK: ECMWF.

Chapman, D. C., & Beardsley, B. C. (1989). On the origin of shelf water in the Middle Atlantic Bight. *Journal of Physical Oceanography*, *19*, 384–391.

Chen, K., & He, R. (2010). Numerical investigation of the middle Atlantic bight shelfbreak frontal circulation using a high-resolution ocean hindcast model. *Journal Physical Oceanography*, *40*, 949–964. https://doi.org/10.1175/2009JPO4262.1

Chen, K., Gawarkiewicz, G., Kwon, Y.-O., & Zhang, W. G. (2015). The role of atmospheric forcing versus ocean advection during the extreme warming of the Northeast U.S. continental shelf in 2012. *Journal of Geophysical Research: Oceans*, *120*, 4324–4339. https://doi.org/10.1002/2014JC010547

Chen, K., Gawarkiewicz, G. G., Lentz, S. J., & Bane, J. M. (2014). Diagnosing the warming of the Northeastern U.S. Coastal Ocean in 2012: A linkage between the atmospheric jet stream variability and ocean response. *Journal of Geophysical Research: Oceans*, *119*, 218–227. https://doi.org/10.1002/2013JC009393

Chen, K., Kwon, Y.-O., & Gawarkiewicz, G. (2016). Interannual variability of winter-spring temperature in the Middle Atlantic Bight: Relative contributions of atmospheric and oceanic processes. *Journal of Geophysical Research: Oceans*, *121*, 4209–4227. https://doi.org/10.1002/2016JC011646

Dai, Y., Feldstein, S. B., Tan, B., & Lee, S. (2017). Formation mechanisms of the Pacific–North American teleconnection with and without its canonical tropical convection pattern. *Journal of Climate*, *30*, 3139–3155.

Emery, W. J., & Thomson, R. E. (2001). Chapter 3: Statistical methods and error handling. In W. J. Emery & R. E. Thomson (Eds.), *Data analysis methods in physical oceanography* (pp. 193–304). New York, NY: Elsevier Science.

Forsyth, J. S. T., Andres, M., & Gawarkiewicz, G. G. (2015). Recent accelerated warming of the continental shelf off New Jersey: Observations from the CMVOleander expendable bathythermograph line. *Journal of Geophysical Research: Oceans*, *120*, 2370–2384. https://doi.org/10.1002/2014JC010516

Fratantoni, P. S., Pickart, R. S., Torres, D. J., & Scotti, A. (2001). Mean structure and dynamics of the shelfbreak jet in the middle Atlantic bight during fall and winter. *Journal of Physical Oceanography*, *31*, 2135–2156.

Greene, C. H., & Pershing, A. J. (2007). Climate drives sea change. *Science*, *315*, 1084–1085.

Hurrell, J. W. (1995). Decadal trends in the north Atlantic oscillation: Regional temperatures and precipitation. *Science*, *269*, 676–679.

Joyce, T. M., & Zhang, R. (2010). On the path of the Gulf Stream and the Atlantic meridional overturning circulation. *Journal of Climate*, *23*, 3146–3154.

Kwon, Y.-O., & Joyce, T. M. (2013). Northern hemisphere winter atmospheric transient eddy heat fluxes and the Gulf Stream and Kuroshio–Oyashio extension variability. *Journal of Climate*, *26*, 9839–9859.

Large, W. G., & Pond, S. (1981). Open ocean momentum flux measurements in moderate to strong winds. *Journal of Physical Oceanography*, *11*, 324–336.

Lentz, S. J. (2008). Observations and a model of the mean circulation over the middle Atlantic bight continental shelf. *Journal of Physical Oceanography*, *38*, 1203–1221.

Linder, C. A., & Gawarkiewicz, G. G. (1998). A climatology of the shelfbreak front in the Middle Atlantic Bight. *Journal of Geophysical Research*, *103*, 18405–18423.

Link, J. S., & Ford, M. D. (2006). Widespread and persistent increase of Ctenophora in the continental shelf ecosystem off NE USA. *Marine Ecology Progress Series*, *320*, 153–159.

Lucey, S. M., & Nye, J. A. (2010). Shifting species assemblages in the Northeast US Continental shelf large marine ecosystem. *Marine Ecology Progress Series*, *415*, 23–33.

Mantua, N. J., Hare, S. R., Zhang, Y., Wallace, J. M., & Francis, R. C. (1997). A Pacific interdecadal climate oscillation with impacts on Salmon production. *Bulletin of the American Meteorological Society*, *78*, 1069–1079.

McKinnon, K. A., Rhines, A., Tingley, M. P., & Huybers, P. (2016). Long-lead predictions of eastern United States hot days from Pacific sea surface temperatures. *Nature Geoscience*, *9*, 389–394.

Mesinger, F., DiMego, G., Kalnay, E., Mitchell, K., Shafran, P. C., Ebisuzaki, W., et al. (2006). North American regional reanalysis. *Bulletin of the American Meteorological Society*, *87*, 343–360.

Mills, K., Pershing, A., Brown, C., Chen, Y., Chiang, F.-S., Holland, D., et al. (2013). Fisheries management in a changing climate: Lessons from the 2012 ocean heat wave in the Northwest Atlantic. *Oceanography*, *26*, 191–195.

Monterey, G., & Levitus, S. (1997). Seasonal variability of mixed layer depth for the world ocean (NOAA Atlas NESDIS, Vol. 14, 100 pp.). Silver Spring, MD: National Oceanic and Atmospheric Administration.

Mountain, D. G. (2012). Labrador slope water entering the Gulf of Maine: Response to the North Atlantic oscillation. *Continental Shelf Research*, *47*, 150–155.

Newman, M., Alexander, M. A., Ault, T. R., Cobb, K. M., Deser, C., Lorenzo, E. D., et al. (2016). The Pacific decadal oscillation, revisited. *Journal of Climate*, *29*, 4399–4427.

Newman, M., Kiladis, G. N., Weickmann, K. M., Ralph, F. M., & Sardeshmukh, P. D. (2012). Relative contributions of synoptic and low-frequency eddies to time-mean atmospheric moisture transport, including the role of atmospheric rivers. *Journal of Climate*, *25*, 7341–7361.

Nye, J. A., Joyce, T. M., Kwon, Y.-O., & Link, J. S. (2011). Silver hake tracks changes in Northwest Atlantic circulation. *Nature Communication*, *2*, 412.

Nye, J. A., Link, J. S., Hare, J. A., & Overholtz, W. J. (2009). Changing spatial distribution of fish stocks in relation to climate and population size on the Northeast United States continental shelf. *Marine Ecology Progress Series*, *393*, 111–129.

Peña-Molino, B., & Joyce, T. M. (2008). Variability in the Slope Water and its relation to the Gulf Stream path. *Geophysical Research Letters*, *35*, L03606. https://doi.org/10.1029/2007GL032183

Pershing, A. J., Alexander, M. A., Hernandez, C. M., Kerr, L. A., Le Bris, A., Mills, K. E., et al. (2015). Slow adaptation in the face of rapid warming leads to collapse of the Gulf of Maine cod fishery. *Science*, *350*, 809–812.

Price, J. F., Weller, R. A., & Pinkel, R. (1986). Diurnal cycling: Observations and models of the upper ocean response to diurnal heating, cooling, and wind mixing. *Journal of Geophysical Research*, *91*, 8411–8427.

Qiu, B., & Kelly, K. A. (1993). Upper-ocean heat balance in the Kuroshio extension region. *Journal of Physical Oceanography*, *23*, 2027–2041.

Reynolds, R. W., Smith, T. M., Liu, C., Chelton, D. B., Casey, K. S., & Schlax, M. G. (2007). Daily High-Resolution-Blended Analyses for Sea Surface Temperature. *Journal of Climate*, *20*, 5473–5496.

Ruprich-Robert, Y., Msadek, R., Castruccio, F., Yeager, S., Delworth, T., & Danabasoglu, G. (2017). Assessing the climate impacts of the observed Atlantic multidecadal variability using the GFDL CM2.1 and NCAR CESM1 global coupled models. *Journal of Climate*, *30*, 2785–2810.

Santos, J. A., Woollings, T., & Pinto, J. G. (2013). Are the winters 2010 and 2012 archetypes exhibiting extreme opposite behavior of the North Atlantic jet stream?. *Monthly Weather Review*, *141*, 3626–3640.

Shearman, R. K., & Lentz, S. J. (2010). Long-term sea surface temperature variability along the U.S. east coast. *Journal of Physical Oceanography*, *40*, 1004–1016.

Vimont, D. J. (2005). The contribution of the interannual ENSO cycle to the spatial pattern of decadal ENSO-like variability. *Journal of Climate*, *18*, 2080–2092.

Wallace, J. M., & Gutzler, D. S. (1981). Teleconnections in the geopotential height field during the northern hemisphere winter. *Monthly Weather Review*, *109*, 784–812.

Walsh, H. J., Richardson, D. E., Marancik, K. E., & Hare, J. A. (2015). Long-term changes in the distributions of larval and adult fish in the northeast U.S. shelf ecosystem. *PLoS One*, *10*, e0137382.

Xu, H., Kim, H.-M., Nye, J. A., & Hameed, S. (2015). Impacts of the north Atlantic oscillation on sea surface temperature on the northeast US continental shelf. *Continental Shelf Research*, *105*, 60–66.

Yu, L., & Weller, R. A. (2007). Objectively analyzed air–sea heat fluxes for the global ice-free oceans (1981–2005). *Bulletin of the American Meteorological Society*, *88*, 527–539.